



# Response of the MIMOSIS-1 CMOS Monolithic Active Pixel Sensor to particle beams with different $dE/dx$

H. Darwish<sup>a,b,\*</sup>, A. Altingun<sup>b</sup>, J. Andary<sup>a</sup>, B. Arnoldi-Meadows<sup>a</sup>, J. Baudot<sup>b</sup>, G. Bertolone<sup>b</sup>, A. Besson<sup>b</sup>, R. Bugiel<sup>b</sup>, G. Claus<sup>b</sup>, C. Colledani<sup>b</sup>, M. Deveau<sup>c</sup>, A. Dorokhov<sup>b</sup>, Z. El Bitar<sup>b</sup>, M. Goffe<sup>b</sup>, A. Himmi<sup>b</sup>, C. Hu-Guo<sup>b</sup>, K. Jaaskelainen<sup>b</sup>, O. Keller<sup>f</sup>, M. Koziel<sup>a</sup>, F. Matejcek<sup>a</sup>, J. Michel<sup>a</sup>, F. Morel<sup>b</sup>, C. Müntz<sup>a</sup>, H. Pham<sup>b</sup>, C.J. Schmidt<sup>c</sup>, M. Specht<sup>b</sup>, J. Stroth<sup>a,c,d</sup>, I. Valin<sup>b</sup>, M. Winter<sup>e</sup>

<sup>a</sup> Goethe-Universität Frankfurt, Max-von-laue-Str. 1, Frankfurt, 60438, Germany

<sup>b</sup> IPHC, Rue de Loess 23, Strasbourg, 67100, France

<sup>c</sup> GSI Helmholtzzentrum für Schwerionenforschung GmbH, Planckstr. 1, Darmstadt, 64291, Germany

<sup>d</sup> Helmholtz Forschungsakademie Hessen für FAIR, Planckstr. 1, Darmstadt, 64291, Germany

<sup>e</sup> IJCLab, 15 Rue Georges Clemenceau, Orsay, 91400, France

<sup>f</sup> Facility for Antiproton and Ion Research in Europe GmbH, Planckstr. 1, Darmstadt, 64291, Germany

## ARTICLE INFO

### Keywords:

CPS  
MAPS  
Tracking detectors  
 $dE/dx$

## ABSTRACT

The ultra-thin and highly granular CMOS Monolithic Active Pixel Sensors (MAPS) are typically optimized for high rate high precision tracking, which implies the use of a very thin active medium and digital readout. Both features hamper using the devices for identifying low momentum particles by means of  $dE/dx$ . Still, MAPS feature charge sharing and typically clusters of more than one fired pixel per impinging particles are formed. It was previously shown that the number of fired pixels per cluster scales with the  $dE/dx$ , which allowed identifying highly ionizing nuclear fragments [1]. Assuming a sufficiently strong response to different  $dE/dx$ , this approach could also be considered for distinguishing minimum ionizing particles (MIP) from light fragments like alpha particles in tracking detectors. In this work, we study this response with particle beams with a  $dE/dx$  of up to four times the ones of MIPs, for non-irradiated and irradiated chips, with different sensing nodes as implemented in the MIMOSIS-1 prototype used for the vertex detector of the CBM experiment.

## 1. Introduction

Particle identification at particle/heavy-ion physics experiments is typically done using dedicated particle identification detectors like TOF and RICH. This may fail for very low momentum particles as they are deflected by the magnetic field of the trackers and thus do not reach dedicated particle identification detectors. Therefore, it is of interest if the tracking detectors can perform standalone particle identification or at least contribute to it. For example, the  $dE/dx$  information provided by tracking detectors like TPCs is used to identify particles. The approach relies on the fact that the energy deposit of particles in matter ( $dE/dx$ ) depends strongly on their velocity according to the Bethe-Bloch-Formula. Combining information on the particle  $dE/dx$ , momentum and charge, allows to estimate the mass and thus identify the particle.

Silicon tracking devices like CMOS Monolithic Active Pixel Sensors (MAPS) are optimized for precision tracking with the least possible

feedback to the particle momentum. This drives the technology towards the highest spatial resolutions and lowest possible material budget. Minimizing this budget motivates using thin active media, which create small signals for Minimum Ionizing Particles (MIPs), that are moreover subjected to strong Landau fluctuations. The requirements on best spatial resolution motivate using small pixels which hampers adding components like ADCs, which would be needed to read out precise  $dE/dx$  information. State-of-the-art MAPS like ALPIDE [2] and MIMOSIS feature in-pixel discriminators, which provide no energy information. This design choice was done in favor of reaching the excellent spatial resolution, time stamping and high rate capability required for the primary task of the sensors. Still, MAPS show charge sharing between individual pixels and clusters of few fired hits per impinging particles may be formed. It was shown that the number of fired pixels in a cluster correlates with the particle  $dE/dx$ , which allows to identify highly ionizing nuclear fragments [1]. We studied if this

\* Correspondence to: 08 rue de Palerme, 67000, Strasbourg, France.

E-mail address: [h.darwish@gsi.de](mailto:h.darwish@gsi.de) (H. Darwish).

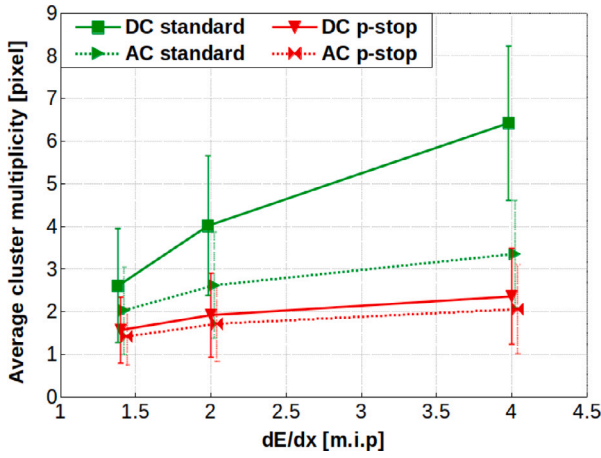


Fig. 1. The average cluster multiplicity as function of the energy deposit of the impinging particles, denoted as multiples of the one of MIPs. The error bars correspond to the RMS of the underlying distribution.

approach would also allow to distinguish light nuclear fragments as frequently observed in heavy ion experiments from MIPs.

## 2. The MIMOSIS-1 sensor

The study was performed with the MIMOSIS-1 prototype designed within the R&D for the Micro Vertex Detector (MVD) [3] of the CBM [4] experiment being built at FAIR. The final sensor will combine a spatial resolution of  $\sigma \approx 5 \mu\text{m}$  and a time resolution of  $\sigma \approx 5 \mu\text{s}$ . Moreover, it has to withstand a peak rate of  $80 \text{ MHz}/\text{cm}^2$  and a combined radiation dose of  $5 \text{ MRad}$  and  $10^{14} \text{ n}_{\text{eq}}/\text{cm}^2$ . MIMOSIS-1 relies on the TJ 180 nm CMOS imaging process with  $25 \mu\text{m}$  thick epitaxial layer and features  $1024 \times 504$  pixels with  $27 \times 30 \mu\text{m}^2$  pitch. It was produced with three different epitaxial layer doping profiles. The “standard” pixel features a point-like  $2 \times 2 \mu\text{m}^2$  n-well implantation forming a collection diode with the p-doped epitaxial layer. The radial field geometry obtained is not suited to fully deplete this layer. Signal charge created in the non-depleted part of the epitaxial layer is collected by diffusion. This slow and undirected process favors high cluster multiplicities and limits the radiation tolerance of the device. Modified pixel structures as discussed in [5] add a deep n-implantation covering most of the pixel surface. This creates a flat field geometry which is anticipated to fully deplete the pixel. The deep n-implantations are either interrupted by a gap (“n-gap”) or an explicitly placed p-implantation (“p-stop”). Despite being slightly different, both options showed rather similar performances in previous tests, thus this work will restrict itself on comparing the “standard” pixel with the “p-stop” pixel. The charge collection diode is DC(AC)-coupled to the amplifier where the top-bias (HV) of the diodes was about  $1.5 \text{ V}$  (DC) and  $10 \text{ V}$  (AC). Moreover, a Back Bias (BB) of  $-1 \text{ V}$  was applied in both cases. The threshold of the sensors was set to  $150e$  as calibrated with a capacitor injecting signal charge to the sensing node. More information on the sensor and this calibration is found in [6,7].

## 3. Experimental setup

The sensors in-beam tests shown were done at CERN-SPS (pion beam) and COSY synchrotron (deuterium beam), using a telescope built with six MIMOSIS-1 chips that were mounted on PCBs and distant by  $1.5 \text{ cm}$  one from each other. The beam was hitting the telescope perpendicular to the DUT. The beam test data was analyzed using TAF analysis package [8]. Hits in the DUTs were associated to tracks reconstructed by the reference planes and the hit cluster multiplicity on the DUT was recorded. Data from CERN with estimated  $120 \text{ GeV}/c$  pions, which

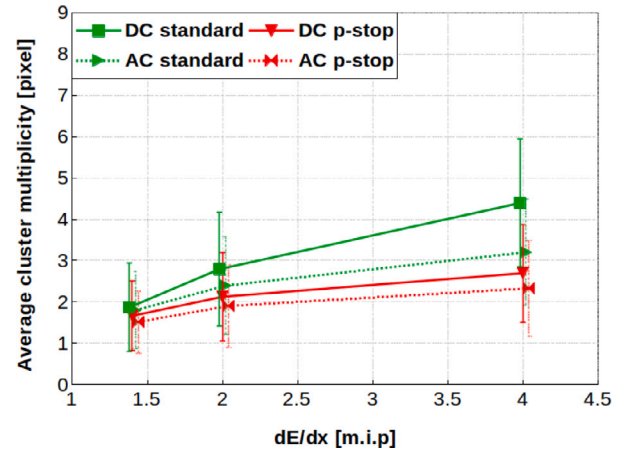


Fig. 2. The average cluster multiplicity as function of the energy deposit of the impinging particles, denoted as multiples of the one of MIPs for combined irradiated sensors ( $5 \text{ MRad} + 10^{14} \text{ n}_{\text{eq}}/\text{cm}^2$ ). The error bars correspond to the RMS of the underlying distribution.

correspond to a  $dE/dx$  of  $\sim 1.4$  times the  $dE/dx$  of MIPs, were used as reference. At COSY, sensors were tested with a deuterium beam with a total beam momentum of  $0.8 \text{ GeV}/c$  or  $1.4 \text{ GeV}/c$ . This corresponds to about four and two times the  $dE/dx$  of a MIP, respectively. Note that the  $0.8 \text{ GeV}/c$  beam provides the same  $dE/dx$  as a nuclear fragment with charge  $z = 2$  and “minimum ionizing” velocity.

Sensors with DC- and AC-coupled pixels on “standard” and “p-stop” epitaxial layer, as introduced previously, were tested. Moreover, we tested sensors, which were irradiated with a  $1 \text{ MeV}$  neutrons at the JSI TRIGA214 reactor in Ljubljana [9], and hereafter exposed to an additional ionizing dose rate of  $\sim 280 \text{ kRad}/h$  of soft X-rays from the  $60 \text{ kV}$  X-ray generator of the Karlsruhe Institute of Technology (KIT). The sensors were irradiated and stored for few months at room temperature. Thus room temperature annealing may have reduced leakage currents [10] and possibly reverted radiation induced threshold shifts. We consider that those known radiation effects have few impact on our study as the leakage current is compensated by device design and the threshold was tuned for the individual sensor.

## 4. Results

The response of the sensors was studied for the different beams and thus as function of the  $dE/dx$ , for chips with both doping profiles (“standard” and “p-stop”) and for the different pixel flavors (DC and AC). Fig. 1 shows the average cluster multiplicity as function of the energy deposit of the impinging particles, denoted as multiples of the one of MIPs, for the different epitaxial layer types (“standard” and “p-stop”) and pixel flavors (DC and AC). The error bars indicate the RMS of the related distribution (see examples more below). The points were slightly shifted on the  $X$ -axis to ease the reading of the error bars.

As expected, the response of the pixels depends strongly on the sensor depletion: the multiplicity of the sensors with a fully depleted “p-stop” epitaxial layer does not vary substantially with the different energy loss cases. This is as the electric fields in the depleted volume direct the additional signal charge carriers to the same few pixels, which receive more charge but are not capable to indicate this. The energy loss dependency is more pronounced for the partially depleted “standard” epitaxial layer. Here, a fraction of the additional signal electrons is not exposed to strong drift fields and diffuses away from the central seed pixel of the cluster towards neighboring pixels. This increases the probability that one of those pixels receives a signal charge above the discriminator threshold and thus the cluster multiplicity. For both “standard” and “p-stop” chips, comparing between DC- and AC-coupled

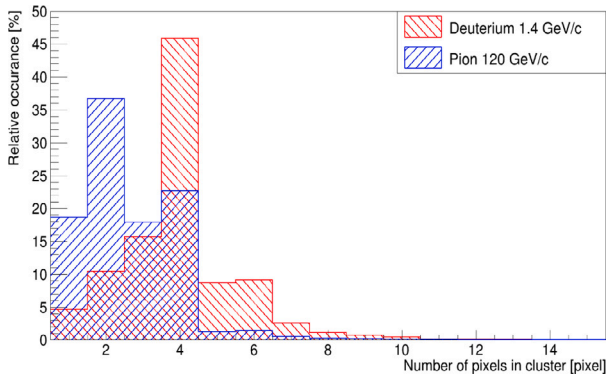


Fig. 3. Distribution of the cluster size of a “standard” epitaxial layer with DC-coupled pixels, obtained experimentally with different particle beams (120 GeV/c pions and 1.4 GeV/c deuteriums) at  $-1V$  BB and  $150e^-$  discriminator threshold.

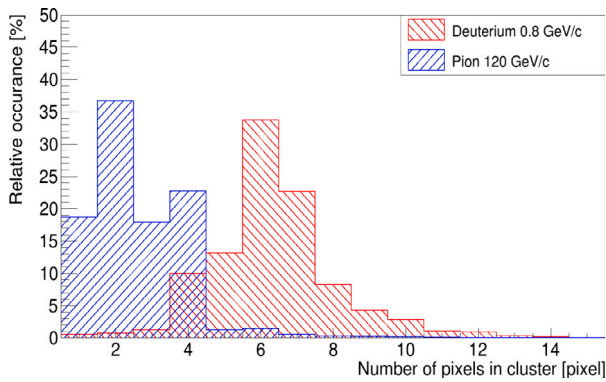


Fig. 4. Distribution of the cluster size of a “standard” epitaxial layer with DC-coupled pixels, obtained experimentally with different particle beams (120 GeV/c pions and 0.8 GeV/c deuteriums) at  $-1V$  BB and  $150e^-$  discriminator threshold.

pixels, the additional 10 V HV applied for the former reduces the cluster multiplicity compared to the latter, as it favors a concentration of the signal charge to the central pixels.

Fig. 2 shows the same plot for sensors irradiated with a combined dose of  $5 \text{ MRad} + 10^{14} n_{eq}/\text{cm}^2$ . One observes the sensors with “standard” epitaxial layer to show an average cluster multiplicity lower than the case of the non-irradiated chips. This was expected as bulk damage caused by the non-ionizing radiation reduces the life-time and such the range of signal electrons diffusing to the cluster periphery [11]. Remarkably, one observes a small opposite trend for “p-stop” type sensors, which remains however in the order of the uncertainties of the underlying measurements.

While the mean value cluster multiplicity increases significantly as a function of the  $dE/dx$ , this fact by its own is of few practical relevance for PID as long as the related distributions strongly overlap. To provide an insight to the overlap, the related distributions are shown for the best (“standard” DC-pixel, not irradiated) and the worst case (“p-stop” AC-pixel, not irradiated) in Figs. 3 to 5, which each compare the distribution for the 120 GeV/c pion beam (in blue //) and the 1.4 GeV/c or 0.8 GeV/c deuterium beam (in red \\\). One observes the standard DC-pixel to provide a visible onset of a separation of the distributions at 1.4 GeV, which gets more pronounced at 0.8 GeV/c. For the “p-stop”-pixel, this separation remains limited even at highest  $dE/dx$ .

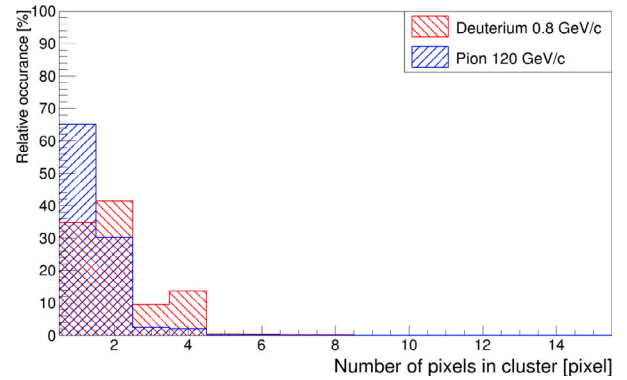


Fig. 5. Distribution of the cluster size of a “p-stop” epitaxial layer with AC-coupled pixels, obtained experimentally with different particle beams (120 GeV/c pions and 0.8 GeV/c deuteriums) at  $-1V$  BB, 10 V HV and  $150e^-$  discriminator threshold.

## 5. Summary and outlook

The first results shown suggest that the MVD may provide a restricted particle identification capability, which may be further improved by combining the information obtained from several sensor layers of a MAPS based tracking system. Best results are observed for lowest sensor depletion and thus for the most radiation soft sensor configuration. The PID potential needs therefore to be traded against the required radiation tolerance. Typically, layers nearby to the interaction point may be configured for best radiation tolerance while PID could rather be performed in more distant layers. The PID capability observed might be improved by using thicker, e.g.  $50 \mu\text{m}$  thick, sensitive layers, which we intend to test with the future MIMOSIS-2 prototype. No quantitative statement on the PID capability is made at this stage as important aspects including the response of the sensors to inclined tracks are still being studied. In a next step, we intend to reproduce the results obtained with a detailed simulation relying on the Allpix<sup>2</sup> framework [12]. The calibrated model will allow to interpolate the measured data points and such pave the way towards more quantitative estimates on the PID capabilities of the sensors.

## Declaration of competing interest

The authors declare that they have no known competing financial interests or personal relationships that could have appeared to influence the work reported in this paper.

## Acknowledgments

Funding: This work was supported by BMBF, Germany, HFHF and Tangerine. We wish to thank our colleagues from CERN and COSY for their valuable support during the data taking.

## References

- [1] C.A. Reidel, et al., Response of the Mimosa-28 pixel sensor to a wide range of ion species and energies, *Nucl. Instrum. Methods A* (2021).
- [2] M. Mager, ALPIDE, the monolithic active pixel sensor for the ALICE ITS upgrade, *Nucl. Instrum. Methods A* (2019).
- [3] J. Stroth, et al., (editors) for the CBM collaboration, Technical Design Report for the CBM: Micro Vertex Detector (MVD), <https://fair-center.eu/user/publications/experiment-collaboration-publications#c56056>.
- [4] T. Ablyazimov, et al., the C.B.M. collaboration, Challenges in QCD matter physics –The scientific program of the Compressed Baryonic Matter experiment at FAIR, <https://doi.org/10.1140/epja/i2017-12248-y>.
- [5] W. Snoeys, et al., A process modification for CMOS monolithic active pixel sensors for enhanced depletion, timing performance and radiation tolerance, *Nucl. Instrum. Methods A* (2017).

- [6] M. Deveaux, et al., Observations on MIMOSIS-0, the first dedicated CPS prototype for the CBM MVD, Nucl. Instrum. Methods A (2020).
- [7] H. Darwish, et al., Tolerance of the MIMOSIS-1 CMOS Monolithic Active Pixel Sensor to ionizing radiation, JINST (2023).
- [8] IPHC-PICSEL group, TAF analysis framework, <https://github.com/jeromebaudot/taf>.
- [9] L. Snoj, et al., Computational analysis of irradiation facilities at the JSI TRIGA reactor, Nucl. Instrum. Methods A (2012).
- [10] D. Doering, et al., Annealing studies on X-ray and neutron irradiated CMOS Monolithic Active Pixel Sensors, Nucl. Instrum. Methods A (2011).
- [11] M. Deveaux, Progress on the radiation tolerance of CMOS Monolithic Active Pixel Sensors, JINST (2019).
- [12] S. Spannagel, et al., Allpix<sup>2</sup>: A modular simulation framework for silicon detectors, Nucl. Instrum. Methods A (2018).